Japanese J. Applied Physics
SAND98-2722J

Stress and Defect Control in GaN Using Low Temperature Interlayers

H. Amano, M. Iwaya, T. Kashima, M. Katsuragcawa and I. Akasaki
Meijo University, Shiogamaguchi, Tempaku-ku, Nagoya 468-8502, Japan

J. Han, S. Hearne, J. A. Floro, E. Chason and J. Figiel
Sandia National Laboratories, Albuquerque, NM 87185-0601, USA
(Received:

Abstract

In organometallic vapor phase epitaxial growth of GaN on sapphire, the role of the low-temperature-deposited interlayers inserted between high-temperature-grown GaN layers was investigated by *in situ* stress measurement, X-ray diffraction, and transmission electron microscopy. Insertion of a series of low temperature GaN interlayers reduces the density of threading dislocations while simultaneously increasing the tensile stress during growth, ultimately resulting in cracking of the GaN film. Low temperature AlN interlayers were found to be effective in suppressing cracking by reducing tensile stress. The interlayer approach permits tailoring of the film stress to optimize film structure and properties.

Keywords; GaN, low temperature deposited layer, stress, strain

1. Introduction

Pioneering work by Maruska and Tietjen [1] and Pankove *et al.* [2] demonstrated the significant potential of GaN as a short wavelength light emitter. However, the difficulty in growing high crystalline quality GaN free of cracks, and in fabricating p-type GaN, have long prevented the practical application of GaN. The use of low-temperature-deposited buffer layer (LT-buffer) [3,4] and the realization of p-type GaN [5,6] triggered the vast expansion of nitride research worldwide [7]. Today, bright blue LEDs and green LEDs based on nitrides

have been commercialized, and purple, deep purple and even UV laser diodes have been fabricated. Microwave FET and solar-blind UV detectors are also available. These results are remarkable considering the 16% lattice mismatch between GaN and sapphire, which were brought about by LT-buffer approach. Nevertheless, GaN grown on sapphire using LT-buffers still contains a high threading dislocations (TDs) densities on the order of 10^8-10^{10}cm^{-2} that originate at the interface between GaN and sapphire [8,9].

Recently, we reported that insertion of low-temperature-deposited GaN (LT-GaN) or AlN (LT-AlN) interlayers between high-temperature-grown GaN (HT-GaN) layers reduces TDs densities [10,11]. However, the mechanism for dislocation reduction has not yet been clarified.

In this study, *in situ* stress monitoring and *ex situ* structural characterization by X-ray diffraction (XRD) and transmission electron microscopy (TEM) were performed to investigate structural properties of GaN as a function of the composition and number of interlayers.

2. Experiments

Nominally undoped GaN layers were grown on (0001) sapphire substrates in a vertical rotating disk reactor [12] or horizontal reactor [13]. TMGa, TMAl and ammonia were used as Ga, Al and nitrogen source gases, respectively, at around 140 Torr growth pressure. In this study, LT-deposition and HT-growth were repeated up to nine times. The thickness of each HT-GaN layer was fixed at ~1 μm. The substrate temperature was ~500 °C for LT deposition of GaN or AlN and 1,050 °C for HT-GaN growth.

The stress at the growth temperature (GT) was determined by measuring the curvature of the sample using the multi-beam optical stress sensor (MOSS) technique, described in detail in ref. 14. Discussion of the real-time stress evolution of GaN during OMVPE growth of GaN

DISCLAIMER

DISCLAIMER

Portions of this document may be illegible in electronic image products. Images are produced from the best available original document.

by MOSS is reported in ref. 15. In this measurement, product of film stress and film thickness was derived from the wafer curvature. For details, see caption of fig.1 and ref.15.

The stress at room temperature (RT) was measured by high resolution X-ray diffraction. $2\theta/\omega$-scans of the (0002) and (20-24) diffraction were used to determine lattice constants c and a at RT [16]. Formula (1) provides an estimate of biaxial stress from the lattice strain:

$$\sigma_{xx} = \frac{(c_{11}+c_{12})*c_{33}-2*c_{13}^{2}}{c_{33}}\varepsilon_{xx} = 449.6\varepsilon_{xx}[GPa]$$
$$= -0.5\frac{(c_{11}+c_{12})*c_{33}-2*c_{13}^{2}}{c_{13}}\varepsilon_{zz} = -883.9\varepsilon_{zz}\ [GPa] \qquad (1)$$

In formula (1), c_{ij} are the elastic constants and ε_{xx} and ε_{zz} are the in-plane and plane-normal lattice strain, respectively. In this paper, values reported in ref. 17 for the c_{ij} of GaN were used.

As a check, the unstrained lattice-constants of a series of GaN films were evaluated from the XRD data. We find $c = 5.1850$ Å and $a = 3.1892$ Å, is in close agreement with the values reported by other groups [18-20]. We also checked the validity of the stress deduced from XRD by comparing the in-plane and plane-normal strains. Differences of stresses deduced from each strain were less than ±0.05 GPa. Plan view transmission electron microscopy (TEM) observation were carried out to measure the density of TDs using a HITACHI H-9000 TEM system with an acceleration voltage of 300 kV. In order to determine the density of TDs of the uppermost layer, the samples were thinned from the back side.

3. Results

The stress of each HT-GaN layer were measured by MOSS at GT, and then measured again at RT by XRD. A compressive thermal stress of 0.67 GPa, due to the difference in thermal shrinkage between GaN and sapphire during cooling from GT to RT, superimposed

onto the growth stress was consistently observed. As pointed out in ref. 15, no measurable lattice relaxation occurred during cooling. Therefore, we can confidently deduce the growth stress from RT strain measurements.

Figure 1 shows traces of substrate temperature, biaxial stress (σ_{xx})-thickness(h_f) product, and TMGa flow into the reactor. The resolution of the stress-thickness plot (0.025 GPa*μm) is limited by wafer thickness, susceptor wobble, electronic noise, etc. As shown in fig.1, the stress during HT-GaN growth can be clearly resolved. During growth of the 1st and 2nd HT-GaN films the stress-thickness product increases linearly, indicating that both HT-GaN layers were grown under a constant tensile stress. We also verified from the reflection intensity monitoring [12] that the growth rate was almost constant during growth except at the very initial growth stage of HT-GaN. From the difference of the initial and final stress-thickness product during growth and thickness of each HT-GaN layer, we deduce the mean tensile stress at GT to be 0.16 GPa and 0.59 GPa during the 1st and 2nd HT-GaN layer growth, respectively. The reason for the sharp rise of the stress-thickness product just after growth of 1st HT-GaN layer is unknown.

The stress measured by MOSS at GT for each HT-GaN layer is plotted in fig.2 (Circle and solid line). Also shown is the RT stress of the top HT-GaN layer for samples grown with varying numbers of interlayers, measured by XRD (Down triangle and dashed line). Since the difference in RT and GT stress in due only to the thermal expansion mismatch of about 0.67 GPa, as previously mentioned [15], we can plot the stress at GT measured by MOSS and stress at RT measured by XRD for different samples in the same figure. For LT-GaN interlayers, a monotonic increase in the tensile stress in the HT-GaN layers over the first three repetitions is consistently observed. XRD stress measurements indicate an increase of 0.3 to 0.4 GPa per interlayer. This is in reasonable agreement with the direct GT stress measurements made by MOSS for the 2 bilayer structure, shown in fig.1. Beyond three

repetitions, the stress at GT saturates at ~1 GPa. The behavior is much different when LT-AlN interlayers are used. In this case, the mean tensile growth stress in each successive HT-GaN layers remains small (about 0.19 GPa) and essentially constant, independent of the number of interlayers deposited.

Figure 3 shows the density of TDs measured by plan view TEM of top HT-GaN layer as a function of number of LT- interlayers. A reduction in the TD density is always observed with an increased number of interlayers. This result is independent of the interlayer material. In other words, both LT-interlayers act as TDs filter.

The apparent scaling of TD density with the mean tensile growth stress observed with LT-GaN interlayers is not found when LT AlN interlayers are used. The origins of the tensile stress during HT-GaN growth and the mechanism of the reduction of TDs with the insertion of LT-interlayers are not well understood and will be discussed in future work. Saturation of the stress at GT above 3 bilayers for the case of LT-GaN interlayers likely results from crack generation when the tensile stress at GT exceeds the yield strength of the material. Figure 4(a) shows an optical micrograph of a crack network in a film with 9 LT-GaN / HT-GaN bilayers. On the contrary, in case of LT-AlN interlayers, cracking is not observed, even in a film with 9 LT-AlN / HT-GaN bilayers (Fig. 4 (b)).

4. Summary

The stress in HT-GaN grown with multiple insertions of low-temperature interlayers was investigated. Large tensile stresses develop in the upper HT-GaN layer in case of LT-GaN interlayers, eventually leading to film cracking. However, use of LT-AlN interlayers suppressed the tensile growth stress. This stress control approach is extremely useful in fabricating thick, low dislocation density GaN films that are free of cracks.

Acknowledgements

The work at Meijo University was partly supported by the Ministry of Education, Science, Sports and Culture of Japan, (contract nos. 09450133, 09875083 and High-Tech Research Center Project), Japan Society for the Promotion of Science (JSPS) Research for the Future Program in the Area of Atomic Scale Surface and Interface Dynamics under the project of "Dynamical Process and Control of Buffer Layer at the Interface in Highly-Mismatched System".

Sandia is a multiprogram laboratory operated by Sandia Corporation, a Lockheed Martin Company, for the United States Department of Energy under Contract DE-AC04-94AL85000.

S.H. would like to acknowledge the support of the US Army Research office under grant DAAH04-96-1-0229.

References

[1] H. P. Maruska and J. J. Tietjen, Appl. Phys. Lett., **15**(1969)327.

[2] J. I. Pankove, E. A. Miller, D. Richman and J. E. Berkeyheiser, J. Lumin., **4**(1971)63.

[3] H. Amano, N. Sawaki, I. Akasaki and Y. Toyoda: Appl. Phys. Lett. **48**(1986) 353.

[4] S. Nakamura, T. Mukai and M. Senoh: J. Appl. Phys. **71**(1992) 5543.

[5] H. Amano, M. Kito, K. Hiramatsu, N. Sawaki and I. Akasaki, Jpn. J. Appl. Phys., **28**(1989)L2112.

[6] S. Nakamura, M. Senoh and T. Mukai, Jpn. J. Appl. Phys., **30**(1992)L1708.

[7] I. Akasaki, Proc. Mater. Res. Soc. **482**(1998)3.

[8] S. D. Lester, F. A. Ponce, M. G. Craford and D. A. Steigerwald, Appl. Phys. Lett., **66**(1995) 1249.

[9] X. J. Ning, F. R. Chien, P. Pirouz, J. W. Yang and M. A. Khan, J. Mater. Res.,

11(1996)580.

[10] M. Iwaya, T. Takeuchi, S. Yamaguchi, C. Wetzel, H. Amano and I. Akasaki: Jpn. .J. Appl. Phys. 37(1998) L316.

[11] M. Iwaya, N. Hayashi, T. Takeuchi, T. Kashima, M. Katsuragwa, H. Kato, S. Yamaguchi, C. Wetzel, H. Amano and I.Akasaki, Jpn. .J. Appl. Phys. (to be submitted).

[12] T. Ng, J. Han, R. Biefled and M. Weckwerth, J. Electron. Mater., 27(1997)190.

[13] K. Hirosawa, K. Hiramatsu, N. Sawaki and I. Akasaki, Jpn. J. Appl. Phys., 32(1993)L1039.

[14] J. Floro, E. Chason, S. Lee, R. Twesten, R. Hwang and L. Freud, J. Electron. Mater., 26(1997)969.

[15] S. Hearne, E. Chason, J. Han, J. Floro, J. Figiel, J. Hunter, H. Amano and I. Tsong, Appl. Phys.Lett., (to be submitted).

[16] For a review, see Optical characterization of epitaxial semiconductor layers, Eds. G. Bauer and W. Richter, Springer, (1996)294 and references therein.

[17] A. Wright, J. Appl. Phys., 82(1997)482.

[18] T. Detchprohm, K. Hiramatsu, K. Itoh and I. Akasaki, Jpn. J. Appl. Phys., 31(1992)L1454.

[19] M. Leszezynski, H. Teisseyre, T. Suski, I. Grzegory, M. Bockowski, J. Jun, S. Porowski, K. Pakula, J. M. Barnowski, C. T. Foxon and T. S. Cheng, Appl. Phys. Lett., 69(1996)73.

[20] W. Rieger, T. Metzger, H. Angerer, R. Dimitrov, O. Ambacher and M. Stutzmann, Appl. Phys. Lett., 68(1996)970.

Figure captions

Fig.1 Traces of substrate temperature, film stress*film thickness (σ_{xx}*h_f) product, and injection of TMGa into the reactor during growth. Product of σ_{xx}*h_f was derived from the wafer curvature using the following equation;

, where, M_s: substrate biaxial Young's modulus, h_s : substrate thickness, κ : wafer curvature $\sigma_{xx} * h_f = \frac{M_s h_s^2}{6} \kappa$ [see ref.15 and references therein]. In this case, one LT-GaN interlayer was inserted between HT-GaN. Therefore, total number of LT-GaN layers is two. The linearity of the stress*thickness during each growth of each HT-GaN layer indicates the presence of a constant tensile stress.

Fig.2 Plot of the stress at GT measured by MOSS of the sample shown in fig.1 (Circle and solid line). The stress at RT measured by XRD, of the top HT-GaN layer, for samples grown with different compositions and numbers of interlayers is also shown. Up-triangles and the dotted line show the LT-AlN case, while down-triangles and the dashed line show the LT-GaN case.

Fig.3 The density of TDs measured by plan view TEM as a function of number of interlayers. Up and down triangles show the LT-AlN and LT-GaN cases, respectively.

Fig.4 (a) Differential interference contrast micrograph of the surface of HT-GaN grown by nine repetitions of the insertion of LT-GaN between HT-GaN. (b) Micrograph of HT-GaN grown by nine repetitions of the insertion of LT-AlN between HT-GaN.

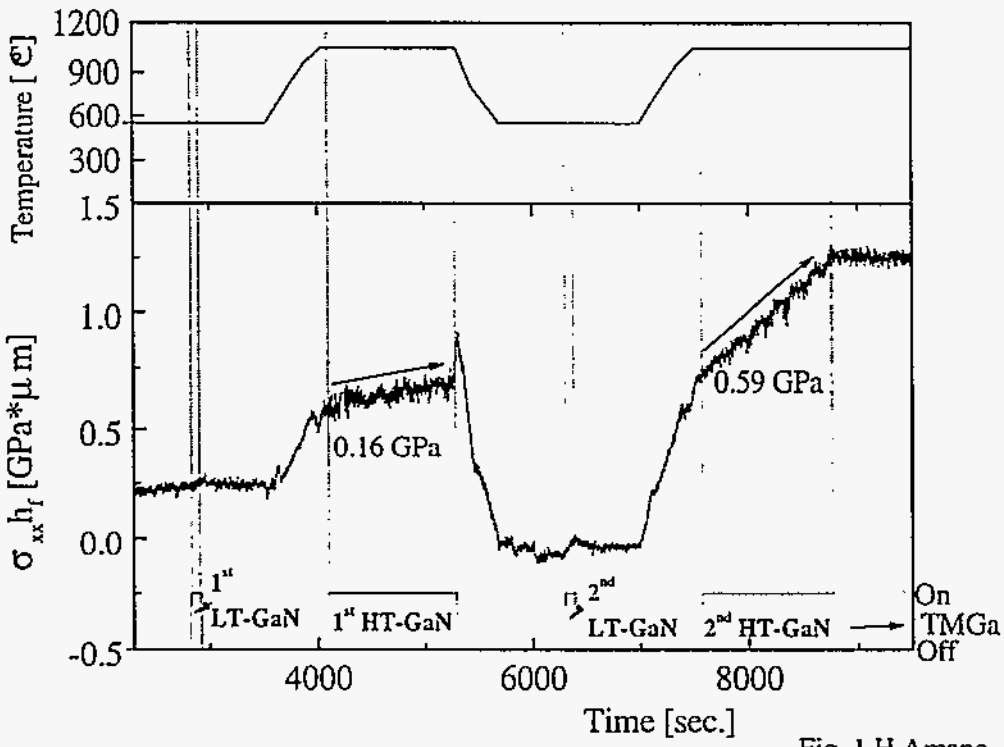
Temperature [℃]
1200
900
600
300
1.5
1.0
0.5
0.0
-0.5
σ xx h f [GPa*μm]
0.16 GPa
0.59 GPa
1st LT-GaN
1st HT-GaN
2nd LT-GaN
2nd HT-GaN
On
TMGa
Off
4000
6000
8000
Time [sec.]

Fig. 1 H Amano

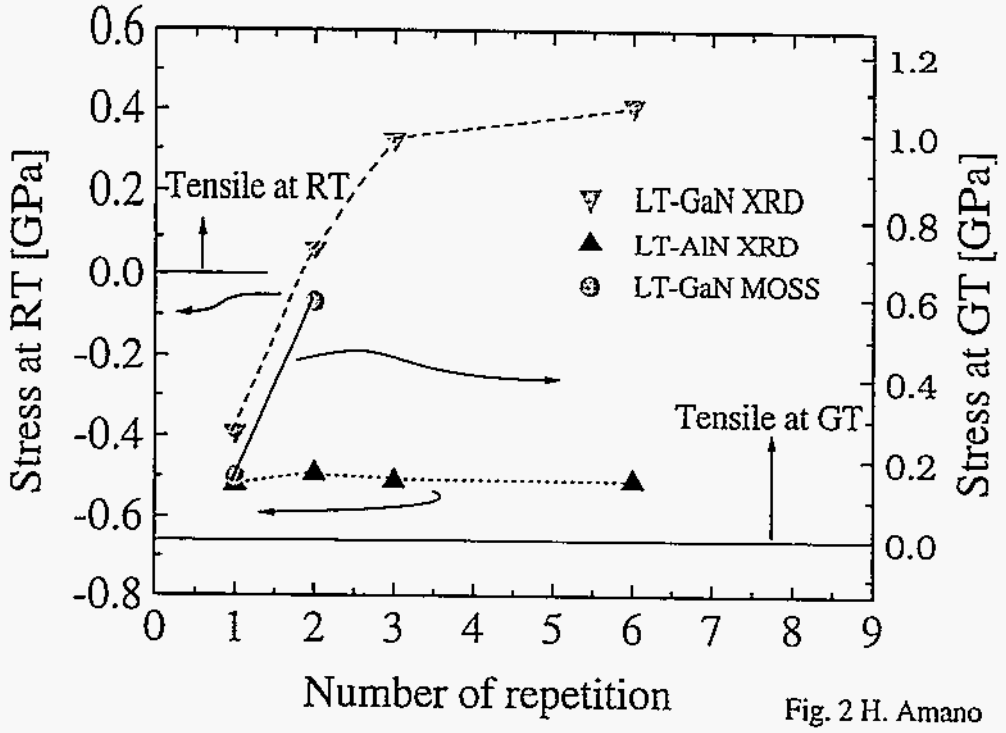
Stress at RT [GPa]
Stress at GT [GPa]
Number of repetition
Tensile at RT
Tensile at GT
LT-GaN XRD
LT-AlN XRD
LT-GaN MOSS
0.6
0.4
0.2
0.0
-0.2
-0.4
-0.6
-0.8
1.2
1.0
0.8
0.6
0.4
0.2
0.0
0
1
2
3
4
5
6
7
8
9

Fig. 2 H. Amano

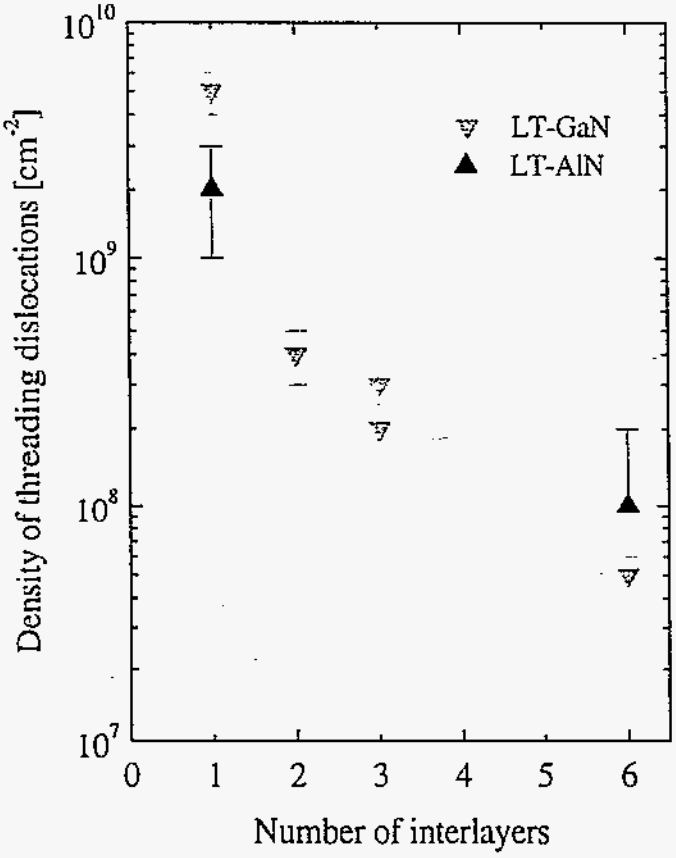
Density of threading dislocations [cm^{-2}]
10^{10}
10^{9}
10^{8}
10^{7}
0
1
2
3
4
5
6
Number of interlayers
LT-GaN
LT-AlN

Fig.3 H. Amano